Band-Gap Character of a Strained Si_4Ge_4[001] Superlattice

Oliver McInnes
L3 Computational physics, Durham
(Dated: March 20, 2026)

The electronic band structure of a strained Si_4Ge_4 [001] superlattice is calculated using an empirical pseudopotential method in a plane-wave basis. The valence-band maximum and conduction-band minimum are identified by a global Brillouin-zone search. The resulting indirect gap is 0.828 eV, between Γ and Γ-X, with a direct gap of 0.972 eV located at Γ. The small 0.144 eV separation between the indirect and direct gaps places the system in a nearly direct regime.

I. INTRODUCTION

Silicon-based semiconductors are foundational to modern electronic technology. However, their extension into optoelectronics is limited by their electronic band structure. Specifically, bulk silicon has an indirect band gap. This makes radiative optical transitions inefficient and limits their usefulness in light-emitting and other photonic devices. As a result, there is considerable interest in engineering silicon-compatible materials with band structures better suited for optical applications.

In a semiconductor, the valence band is filled with electrons at low temperature, while the conduction band is initially empty and separated from the valence band by an energy gap known as the "band gap," which is the minimum energy needed for an electron to move from the valence band to the conduction band. The size and the nature of this gap, whether it is direct (where the highest energy point in the valence band and the lowest in the conduction band have the same crystal momentum) or indirect (where these points occur at different momenta), significantly affect electronic and optical properties. In direct-gap materials, optical transitions between these states do not require a change in momentum, making processes such as light emission efficient. In indirect-gap materials, a phonon is typically required to conserve momentum, reducing the efficiency of light emission and absorption. [1, 2]

One way to modify the band structure of silicon-based materials is through semiconductor superlattices. A superlattice is a structure made by stacking very thin layers of two different semiconductor materials in a repeating, ordered pattern. This setup introduces a larger real-space periodicity in the crystal. As a result, the potential experienced by the electrons is changed. This can lead to an electronic structure that differs from that of the individual bulk materials.

Two effects are especially important in such systems. First, the larger real-space periodicity reduces the size of the Brillouin zone. This reduction causes zone folding, which can bring states from different regions of the bulk band structure into closer proximity in reciprocal space. As a result, an originally indirect gap can behave more like a direct one, and folded transitions may occur at symmetry points such as Γ or M. [3–5] Second, when the layered structure is grown coherently, lattice mismatch between the constituent materials, or constraints from the substrate, can produce strain. In turn, this strain alters interatomic spacing and shifts band energies.[3–5]

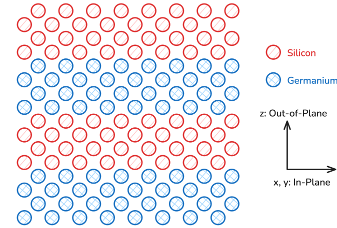

FIG. 1. Schematic of the Si_4Ge_4 [001] superlattice geometry considered here. Silicon and germanium monolayers alternate along the z direction. One superlattice period contains four Si monolayers followed by four Ge monolayers.

The Si/Ge superlattice is of particular interest, because Si and Ge are chemically similar and have closely matched lattice constants, allowing for coherent layered growth. It is also compatible with existing silicon device technology. Certain Si/Ge lattice geometries have been found to exhibit nearly direct optical transitions, making them promising for optoelectronic and high-speed applications.[3–5]

An important aspect of superlattices is strain. Specifically, when a thin crystal layer is grown on a substrate with a different lattice constant, the layer is forced to adopt the substrate's in-plane spacing. This produces a biaxial strain and a corresponding relaxation of the out-of-plane lattice parameter. This strain changes the lattice spacing, modifying the crystal potential and therefore shifting the band energies.[3–5]

In this report, the electronic band structure of a Si_4Ge_4 [001] superlattice is calculated by solving the single-particle Schrödinger equation in a plane-wave basis using an empirical pseudopotential. The electronic states are treated as Bloch waves in the periodic superlattice potential, and the resulting eigenvalue problem is solved numerically to obtain $E_n(\mathbf{k})$.

From the calculated dispersion relation, we extract the material's electronic properties, including the size and character of the band gap. With these quantities, we can then evaluate how the layered Si/Ge structure differs from bulk silicon and determine whether the superlattice geometry yields features of potential use in electronic or

optoelectronic applications.

Therefore, the aim of this work is to determine the size and character of the band gap in a strained Si_4Ge_4 [001] superlattice and to assess whether zone folding and strain drive the system towards direct-gap behaviour.

II. METHODS

To determine how the Si/Ge superlattice geometry modifies the electronic structure, the band dispersion is calculated by solving the single-particle Schrödinger equation for electrons moving in a periodic crystal potential,

$$\left[-\frac{\hbar^2}{2m}\nabla^2 + V(\mathbf{r})\right]\psi(\mathbf{r}) = E\psi(\mathbf{r}), \tag{1}$$

where $V(\mathbf{r})$ is the crystal potential.

In a real solid, this potential is produced by the atomic nuclei and surrounding electrons, and it varies strongly near the nuclei. However, solving the full many-electron problem for a strained supercell is not practical here. Therefore, the crystal is described using an empirical pseudopotential. This approximation replaces the strongly varying ionic potential with a smoother fitted potential that reproduces the relevant band-structure features.[6]

Since the superlattice is periodic, the electronic eigenstates satisfy Bloch's theorem and can be written in the form

$$\psi_{n\mathbf{k}}(\mathbf{r}) = e^{i\mathbf{k}\cdot\mathbf{r}}u_{n\mathbf{k}}(\mathbf{r}), \tag{2}$$

where $u_{n\mathbf{k}}(\mathbf{r})$ has the periodicity of the superlattice, n is the band index, and $\mathbf{k}$ is the crystal wavevector. The Bloch wavefunction is expanded in a plane-wave basis over reciprocal lattice vectors $\mathbf{G}$,

$$\psi_{n\mathbf{k}}(\mathbf{r}) = \sum_{\mathbf{G}} c_{\mathbf{G}}^{(n)} e^{i(\mathbf{k}+\mathbf{G})\cdot\mathbf{r}}. \tag{3}$$

Substituting this expansion into the Schrödinger equation converts the problem into a matrix eigenvalue equation,

$$\sum_{\mathbf{G}'} H_{\mathbf{G},\mathbf{G}'}(\mathbf{k})\, c_{\mathbf{G}'}^{(n)} = E_n(\mathbf{k})\, c_{\mathbf{G}}^{(n)}, \tag{4}$$

where the Hamiltonian matrix elements are

$$H_{\mathbf{G},\mathbf{G}'}(\mathbf{k}) = \frac{\hbar^2}{2m}\left|\mathbf{k}+\mathbf{G}\right|^2 \delta_{\mathbf{G},\mathbf{G}'} + V_{\mathbf{G}-\mathbf{G}'}. \tag{5}$$

The first term is the kinetic energy in the plane-wave basis, while the second describes coupling between basis states through the crystal potential.

The Fourier components of the potential are written in a species-resolved form,

$$V_{\mathbf{G}-\mathbf{G}'} = \frac{1}{\Omega}\sum_{\alpha\in\{\mathrm{Si},\mathrm{Ge}\}} v_\alpha(|\mathbf{G}-\mathbf{G}'|)\, S_\alpha(\mathbf{G}-\mathbf{G}'), \tag{6}$$

where Ω is the supercell volume, $v_\alpha(G)$ is the empirical form factor for species α, and S_α is the corresponding structure factor,

$$S_\alpha(\mathbf{G}-\mathbf{G}') = \sum_{j\in\alpha}\exp[-i(\mathbf{G}-\mathbf{G}')\cdot\mathbf{R}_j]\,. \tag{7}$$

In this, $\mathbf{R}_j$ denotes the atomic position of atom j, and the sum runs over all atoms of species α within the supercell.

The species-dependent pseudopotential form factor is taken to be[6]

$$v_\alpha(G) = \frac{a_1(G^2-a_2)}{e^{a_3(G^2-a_4)}+1}\left[\frac{1}{2}\tanh\left(\frac{a_5-G^2}{a_6}\right)+\frac{1}{2}\right], \tag{8}$$

where the parameters $(a_1,\ldots,a_6)$ are chosen separately for Si and Ge. The values used in this work are listed in Table I.

To form a finite basis of reciprocal lattice vectors (RLVs), only vectors satisfying $|\mathbf{G}| \le G_{\mathrm{cut}}$ are retained. The basis size n_G therefore increases discretely as G_{cut} is raised. Convergence with respect to this cutoff is assessed in Sec. III A.

The Si/Ge [001] superlattice is constructed as a stack of individual [001] monolayers. In the xy-plane, a 1×1 conventional-cell surface unit is used, and each monolayer contains two atoms. The stacking sequence follows the diamond structure and repeats every four layers. In this notation, a Si_4Ge_4 superlattice denotes four consecutive Si monolayers followed by four Ge monolayers, after which the pattern repeats periodically along the growth direction. This layer sequence is shown schematically in Fig. 1.

To model coherent strain relative to a Si substrate, the in-plane lattice constant is fixed to the substrate value $a_\parallel$, so each layer is constrained laterally to match the substrate. The out-of-plane lattice constant is then allowed to relax elastically. For a material with bulk cubic lattice constant a_0 and elastic constants c_{11} and c_{12}, the biaxial strain components under the condition $\sigma_{zz}=0$ are

$$\epsilon_{xx} = \epsilon_{yy} = \frac{a_\parallel}{a_0} - 1, \tag{9}$$

$$\epsilon_{zz} = -2\frac{c_{12}}{c_{11}}\epsilon_{xx}. \tag{10}$$

The corresponding strained out-of-plane lattice parameter is

$$c = a_0(1+\epsilon_{zz}), \tag{11}$$

TABLE I. Empirical pseudopotential parameters used for each species.

Species	a_1	a_2	a_3	a_4	a_5	a_6
Si	106.0686	2.2278	0.6060	-1.9720	5.0	0.3
Ge	54.4512	2.3592	0.7400	-0.3800	5.0	0.3

so that the monolayer spacing for that material is

$$d = \frac{c}{4}. \tag{12}$$

The vertical coordinate of each atomic layer is then obtained by summing the monolayer spacings of all lower layers in the superlattice period. This is therefore a layer-wise linear-elastic approximation. Each monolayer is assigned the spacing implied by the bulk elastic constants, and no additional local interface relaxation beyond the imposed monolayer geometry is included.

For the Si-substrate geometry considered here, the in-plane lattice constant is taken to be the bulk Si value. The Ge layers are therefore strained coherently to the Si in-plane spacing, while the Si layers remain unstrained in-plane.[3] The elastic constants used in the strain model are listed in Table II.

Once the atomic positions and species-dependent pseudopotentials have been defined, the Hamiltonian matrix is assembled for each **k**-point in the chosen reciprocal-space path and diagonalised numerically. The resulting eigenvalues $E_n(\mathbf{k})$ give the band structure plotted in the main figures. To identify the true valence-band maximum (VBM) and conduction-band minimum (CBM), a separate global Brillouin-zone search was performed using a grid search, in case either the VBM or CBM occurs not along a high-symmetry path.

III. RESULTS

A. Convergence

We carried out a convergence test to determine a suitable value for the plane-wave cutoff G_{cut}. For each cutoff, we recorded the corresponding basis size and the resulting Γ-point gap. The full sweep, including the time cost per k-point, is reported in Appendix Table IV.

We found that the convergence is not strictly monotonic. Specifically, the value obtained at $G_{\text{cut}} = 5.25$ Å^{-1} lies closer to the reference value at 7.0 Å^{-1} than several of the intermediate cutoffs. This is likely due to the discrete way that RLVs are added to the plane-wave basis, as the cutoff is increased.

From these results, we select $G_{\text{cut}} = 6.25$ Å^{-1} as the working cutoff for our calculations. At this value, the Γ-point gap differs from the 7.0 Å^{-1} reference result by only 0.045 meV, while keeping the basis size to $n_G = 1391$.

TABLE II. Elastic constants used for the coherent-strain model, taken from the Ioffe Institute semiconductor database [7, 8].

Species	c_{11} (GPa)	c_{12} (GPa)
Si	166.0	64.0
Ge	126.0	44.0

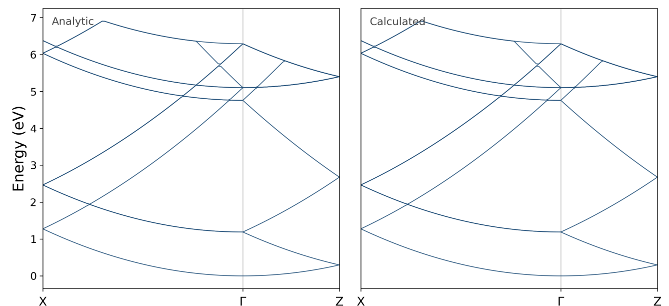

FIG. 2. Free-electron verification along the zone-boundary-centre-zone-boundary path X-Γ-Z. The left panel shows the analytic free-electron branches $E = \hbar^2|\mathbf{k}+\mathbf{G}|^2/2m$, while the right panel shows the eigenvalues obtained from the plane-wave code with the crystal potential set to zero.

This provides a safe compromise between numerical accuracy and computational cost.

We note that the uncertainties in this approach are predominantly systematic. Repeated calculations with fixed parameters were found to be numerically stable, to machine precision. As a result, the dominant source of error in the model is due to controllable approximations, specifically the plane-wave basis truncation.

B. Verification

As a basic verification of the plane-wave implementation, the code was tested in the free-electron limit by setting the crystal potential to zero, $V(\mathbf{r}) = 0$. In this case, the Hamiltonian becomes diagonal in the plane-wave basis, and the eigenvalues should reduce to the analytic free-electron dispersion

$$E(\mathbf{k}+\mathbf{G}) = \frac{\hbar^2}{2m}|\mathbf{k}+\mathbf{G}|^2. \tag{13}$$

This confirms that the kinetic term, RLV generation, and diagonalisation are all implemented correctly.

Fig. 2 compares the analytic and numerical band structures along the X-Γ-Z path. The two are visually indistinguishable. The maximum absolute difference between the numerical and analytic eigenvalues was 0.0 eV to the displayed precision, and the root-mean-square difference over all sampled bands and k-points was likewise 0.0 eV, indicating agreement to machine precision of the numerical implementation. This confirms that the plane-wave basis and Hamiltonian construction behave as expected.

C. Comparison with bulk Si and Ge

To give context to the superlattice results, we carried out calculations for Si and Ge within the same empirical pseudopotential framework and with the same plane-wave cutoff as used for the Si_4Ge_4 [001] structure. This

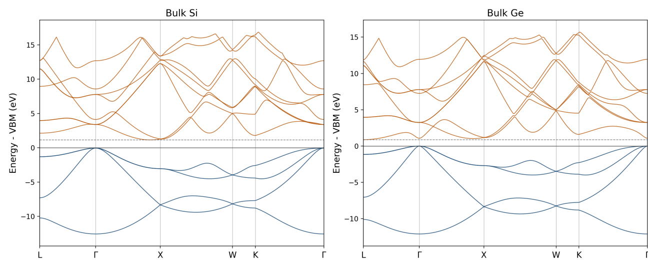

FIG. 3. Calculated bulk Si and bulk Ge band structures, plotted relative to the valence-band maximum. The high-symmetry path follows L-Γ-X-W-K-Γ.

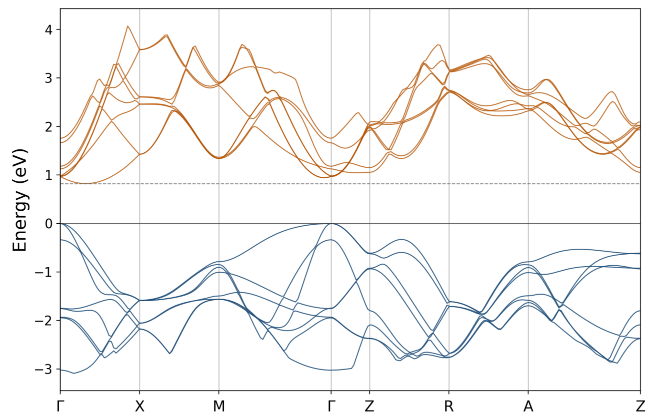

FIG. 4. Calculated band structure of the strained Si_4Ge_4 [001] superlattice, plotted relative to the valence-band maximum. The horizontal axis follows the k-space path Γ-X-M-Γ-Z-R-A-Z.

provides a reference for how strongly the superlattice modifies the band-gap character with respect to its constituents. The corresponding bulk band structures are shown in Fig. 3.

Bulk silicon reproduces the expected behaviour of a strongly indirect semiconductor. The valence-band maximum (VBM) is found at Γ, while the conduction-band minimum (CBM) lies along the Γ–X direction. The resulting indirect gap is 1.147 eV, while the lowest direct transition at Γ is much larger, at 3.434 eV. This is in good agreement with standard literature values, which place the indirect gap near 1.12 eV at room temperature and the direct Γ-point transition near 3.4 eV [9].

Bulk germanium is also reproduced as an indirect semiconductor. The VBM is again found at Γ, while the CBM lies at L in the FCC Brillouin zone. The indirect gap was found to be 0.879 eV, while the direct Γ-point gap is 1.077 eV. These values are somewhat larger than standard literature values for Ge, for which the indirect and direct gaps are typically quoted as approximately 0.66 eV and 0.80 eV, respectively, at room temperature [10]. Regardless, the calculation correctly reproduces the ordering of the band extrema and the fact that Ge is much closer to direct-gap behaviour than Si.

D. Electronic Structure

The calculated band structure of the Si_4Ge_4 [001] superlattice is shown in Fig. 4.

The structure consists of four Si monolayers, followed by four Ge monolayers in each period, and is modelled coherently on a Si substrate, so that the in-plane lattice constant is fixed at $a_\parallel = 5.430$ Å. In this geometry, the supercell contains 16 atoms and has a total period of $c = 11.234$ Å.

TABLE III. Calculated bulk band-gap properties of Si and Ge within the present empirical pseudopotential model. The quantity $\Delta E = E_\Gamma^{\text{dir}} - E_g^{\text{ind}}$ measures the separation between the lowest direct transition at Γ and the indirect gap.

Material	E_g^{ind} (eV)	E_Γ^{dir} (eV)	ΔE (eV)
Si	1.147	3.434	2.287
Ge	0.879	1.077	0.198

The electronic structure is obtained using a plane-wave basis cutoff $G_{\text{cut}} = 6.25$ Å^{-1}, corresponding to $n_G = 1391$ plane waves, and the bands are evaluated along the high-symmetry path Γ-X-M-Γ-Z-R-A-Z.

Under the coherent strain model, the Si layers remain unstrained in-plane because the substrate lattice constant is taken to be the bulk Si value. The Ge layers are then compressed in-plane to match the Si substrate and therefore expand along the growth direction. Using Eqs. (9)–(12), the Ge layers have in-plane strain $\epsilon_\parallel = -0.0389$ and out-of-plane strain $\epsilon_{zz} = +0.0272$, giving a strained out-of-plane lattice parameter $c = 5.804$ Å and monolayer spacing $d = 1.451$ Å. This is the expected substrate-constrained distortion: in-plane compression accompanied by out-of-plane expansion.

The path was sampled from 250 points, and a separate global Brillouin-zone grid search was used to locate the band extrema. The valence-band maximum is found at Γ, with energy $E_{\text{VBM}} = -0.584$ eV. The conduction-band minimum lies slightly away from Γ along the Γ-X direction at $\mathbf{k} = (0.1615, 0, 0)$, with energy $E_{\text{CBM}} = 0.244$ eV. The resulting indirect gap is therefore 0.828 eV.

Although the extrema in the present case occur on the plotted high-symmetry path, the separate Brillouin-zone grid search provides a useful check that the true band edges have been identified. This is helpful in superlattice calculations, where shallow extrema are not guaranteed to be obvious from a symmetry-path plot alone.

The lowest direct transition at Γ occurs at 0.972 eV, only 0.144 eV above the indirect gap. The main result is therefore that the strained Si_4Ge_4 [001] superlattice remains indirectly gapped, but lies close to the direct-gap limit.

Additional higher-energy features in the spectrum are qualitatively consistent with the expected zone-folding

effects of the superlattice periodicity. Since the present work is focused on the fundamental band gap, these higher-energy states are not analysed in detail here.

IV. DISCUSSION

A. Near-direct Character

The main result demonstrates that the strained Si_4Ge_4 [001] superlattice remains indirectly gapped, with the lowest direct Γ-point transition only 0.144 eV higher. This positions the system firmly within a nearly-direct regime.

The global Brillouin-zone search gives an indirect gap of 0.828 eV, with the valence band at Γ and the conduction-band minimum displaced slightly from Γ along the Γ-X direction. The direct Γ-Γ gap is 0.972 eV.

Although this small separation is promising for optoelectronic applications, energetic proximity to a direct gap does not guarantee strong optical transitions. Verifying this requires calculating optical matrix elements and oscillator strengths, which was not done here.

These results align with the main literature values for short-period Si/Ge superlattices. Specifically, the direct Γ-Γ gap found here, 0.972 eV, is very close to the 0.96 eV direct gap reported by Friedel *et al.* in a local empirical pseudopotential calculation.[6]

For the indirect gap, the present value of 0.828 eV is close to the 0.85 eV result reported by Hybertsen and Schlüter and the 0.88 eV experimental gap measured by Olajos *et al.* for short-period Si_4/Ge_4 superlattices.[3, 11]

Together, these findings confirm that the present method reproduces the expected near-gap energy scale and aligns with the consensus that short-period strained Si/Ge superlattices can achieve nearly direct band gaps.[3–5]

B. Comparison with bulk Si and Ge

We can compare the superlattice results with the calculated results from the bulk constituents. Specifically, the separation

$$\Delta E = E_\Gamma^{\mathrm{dir}} - E_g^{\mathrm{ind}}$$

is a useful metric for the directness of the transition. In bulk Si, this separation is very large (2.287 eV), reflecting its strongly indirect character. In bulk Ge, the separation is much smaller (0.198 eV), consistent with the fact that Ge lies relatively close to direct-gap behaviour. However, in the Si_4Ge_4 superlattice, we observe an even smaller value, $\Delta E = 0.144$ eV. This shows that the superlattice is far more direct-like than bulk Si, and even slightly closer to the direct-gap limit than bulk Ge.

This shows that the superlattice's properties cannot be described by a combination of the properties of bulk Si and bulk Ge. The imposed layering introduces a new periodicity along the growth direction, folding bulk-derived states into the reduced superlattice Brillouin zone and giving rise to features absent in the bulk constituents.

C. Limitations

This model, however, has some limitations. The empirical pseudopotential is fitted to bulk band structures and replaces the strongly varying ionic potential with a smoother effective potential, so any interface-specific chemistry, charge redistribution, and other non-bulk effects are only captured approximately.

The larger discrepancy for bulk Ge likely reflects, at least in part, the simplified local pseudopotential treatment and the omission of effects such as spin-orbit coupling, temperature renormalisation, and local interface relaxation, which are important in Ge-rich states.

In addition, strain is treated using a layerwise linear-elastic model. Each monolayer's spacing is defined by the bulk elastic constants under coherent biaxial strain, but no additional local interface relaxation, reconstruction, or intermixing is included. In a real structure, such effects could modify the ordering and energies of the near-edge states.

There are also numerical limitations. Although the plane-wave cutoff was carefully converged for the Γ-point gap, small energy differences between nearby conduction states may still be somewhat sensitive to basis size, k-space sampling, and the details of the extremum search. The main conclusion that the system is indirectly gapped but close to direct-gap behaviour appears robust, but the exact direct-indirect separation should still be interpreted within the accuracy of the present model.

Within these limitations, the present calculation supports the interpretation that a strained Si_4Ge_4 [001] superlattice can exhibit substantially more direct-like electronic behaviour than bulk Si.

V. CONCLUSION

In this work, the electronic band structure of a strained Si_4Ge_4 [001] superlattice on a Si substrate was computed using an empirical pseudopotential method in a plane-wave basis, with the band extrema identified by a separate global Brillouin-zone search. After convergence testing and free-electron verification, the production calculation was performed at $G_{\text{cut}} = 6.25\ \text{Å}^{-1}$.

The central numerical result is an indirect gap of 0.828 eV, with the valence-band maximum at Γ and the conduction-band minimum slightly displaced along Γ-X. The lowest direct transition at Γ is 0.972 eV, only 0.144 eV higher.

Even though the superlattice remains formally indirect, the small 0.144 eV separation from the direct Γ-point transition is still significant. In bulk Si, the lowest direct transition lies much higher above the fundamental gap, so near-edge optical processes are strongly limited by the indirect-gap character. However, in the superlattice, the direct transition lies much closer in energy, suggesting more direct-like optical behaviour than in bulk Si.

The physical implication is that this short-period strained Si/Ge superlattice remains indirect, but lies close to the direct-gap limit. That makes it a useful example of how strain and zone folding can push a silicon heterostructure towards more favourable electronic behaviour.

In further work we should calculate optical matrix elements and oscillator strengths to determine whether the near-direct electronic structure here leads to strong radiative transitions. It would also be useful to include spin-orbit coupling and more realistic interface relaxation, since these effects are relevant to Ge-rich states. Finally, varying the layer thickness and strain state could identify which Si/Ge superlattice geometries most closely approach the direct-gap limit.

REFERENCES

[1] J. Noffsinger, E. Kioupakis, C. G. Van de Walle, S. G. Louie, and M. L. Cohen, Phys. Rev. Lett. **108**, 167402 (2012), DOI: 10.1103/PhysRevLett.108.167402.

[2] M. Zacharias, C. E. Patrick, and F. Giustino, Phys. Rev. Lett. **115**, 177401 (2015), DOI: 10.1103/PhysRevLett.115.177401.

[3] M. S. Hybertsen and M. Schlüter, Phys. Rev. B **36**, 9683 (1987), DOI: 10.1103/PhysRevB.36.9683.

[4] S. Froyen, D. M. Wood, and A. Zunger, Phys. Rev. B **37**, 6893 (1988), DOI: 10.1103/PhysRevB.37.6893.

[5] S. Froyen, D. Wood, and A. Zunger, Thin Solid Films **183**, 33 (1989), DOI: 10.1016/0040-6090(89)90427-6.

[6] P. Friedel, M. S. Hybertsen, and M. Schlüter, Phys. Rev. B **39**, 7974 (1989), DOI: 10.1103/PhysRevB.39.7974.

[7] Ioffe Institute, Silicon, Mechanical properties, elastic constants, lattice vibrations of silicon (si), `https://www.ioffe.ru/SVA/NSM/Semicond/Si/mechanic.html` (2026).

[8] Ioffe Institute, Germanium, Mechanical properties, elastic constants, lattice vibrations of germanium (ge), `https://www.ioffe.ru/SVA/NSM/Semicond/Ge/mechanic.html` (2026).

[9] Ioffe Institute, Nsm archive – band structure and carrier concentration of silicon (si), `https://www.ioffe.ru/SVA/NSM//Semicond/Si/bandstr.html` (2026).

[10] Ioffe Institute, Nsm archive – band structure and carrier concentration of germanium (ge), `https://www.ioffe.ru/SVA/NSM/Semicond/Ge/bandstr.html` (2026).

[11] J. Olajos, J. Engvall, H. G. Grimmeiss, U. Menczigar, G. Abstreiter, H. Kibbel, E. Kasper, and H. Presting, Phys. Rev. B **46**, 12857 (1992), DOI: 10.1103/PhysRevB.46.12857.

VI. GENERATIVE AI STATEMENT

Grammarly was used to correct spelling and grammar. Otherwise, no generative AI has been used in this report.

LAY SUMMARY

This project studied how stacking very thin layers of silicon and germanium changes the electronic structure of the material. Ordinary silicon is excellent for electronics, but it is not very good at emitting light because it has an indirect band gap. One idea is to combine silicon and germanium in a layered superlattice so that the band structure is reshaped by the new crystal periodicity and by strain between the layers.

Using a numerical band-structure calculation, we found that the Si_4Ge_4 superlattice still has an indirect gap, but the lowest direct transition is only 0.144 eV higher in energy. In other words, it is not fully direct-gap, but it is quite close. This makes the material more promising for optical and photonic applications than bulk silicon, and shows how strain and superlattice design can be used to tune the properties of silicon-compatible materials.

Appendix A: Convergence Testing

Table IV summarises the convergence of the Γ-point gap with respect to the plane-wave cutoff.

TABLE IV. Convergence of the calculated Γ-point gap with plane-wave cutoff. The final column gives the absolute difference from the $G_{\mathrm{cut}} = 7.0$ Å^{-1} reference value.

G_{cut} (Å^{-1})	n_G	Gap (eV)	$\lvert\Delta\rvert$ (meV)	Time per point (s)
5.00	693	0.92880584	43.495	0.17
5.25	823	0.97152148	0.779	0.24
5.50	927	0.96121953	11.081	0.31
5.75	1041	0.96930901	2.992	0.40
6.00	1189	0.96891928	3.381	0.52
6.25	1391	0.97225506	0.045	0.74
6.50	1535	0.97223541	0.065	0.98
6.75	1709	0.97218580	0.115	1.34
7.00	1921	0.97230053	0.000	2.04

Appendix B: High-Symmetry Points

The band structure in the main text is evaluated along the reduced-zone path

$$\Gamma - X - M - \Gamma - Z - R - A - Z,$$

using the reduced reciprocal coordinates listed in Table V.

TABLE V. High-symmetry points used for the band-structure path, given in reduced reciprocal coordinates.

Point	Reduced coordinates
Γ	$(0, 0, 0)$
X	$\left(\frac{1}{2}, 0, 0\right)$
M	$\left(\frac{1}{2}, \frac{1}{2}, 0\right)$
Z	$\left(0, 0, \frac{1}{2}\right)$
R	$\left(\frac{1}{2}, 0, \frac{1}{2}\right)$
A	$\left(\frac{1}{2}, \frac{1}{2}, \frac{1}{2}\right)$